Geomechanics and Engineering, *Vol. 13, No. 5 (2017) 743-756*
DOI: https://doi.org/10.12989/gae.2017.13.5.743

A strain hardening model for the stress-path-dependent shear behavior of rockfills

Ming Xu*, Erxiang Song[a] and Dehai Jin[b]

Department of Civil Engineering, Tsinghua University, Beijing 100084, China

(*Received October 12, 2016, Revised April 13, 2017, Accepted May 11, 2017*)

Abstract. Laboratory investigation reveals that rockfills exhibit significant stress-path-dependent behavior during shearing, therefore realistic prediction of deformation of rockfill structures requires suitable constitutive models to properly reproduce such behavior. This paper evaluates the capability of a strain hardening model proposed by the authors, by comparing simulation results with large-scale triaxial stress-path test results. Despite of its simplicity, the model can simulate essential aspects of the shear behavior of rockfills, including the non-linear stress-strain relationship, the stress-dependence of the stiffness, the non-linear strength behavior, and the shearing contraction and dilatancy. More importantly, the model is shown to predict the markedly different stress-strain and volumetric behavior along various loading paths with fair accuracy. All parameters required for the model can be derived entirely from the results of conventional large triaxial tests with constant confining pressures.

Keywords: rockfills; stress path; shear behavior; strain hardening; volumetric change

1. Introduction

Rockfill has been extensively used for the construction of dams and embankments, which have become increasingly high and complex during the past decades (Charles 2008). Stability of such rockfill structures used to be the predominant consideration (e.g., Griffiths and Marquez 2007, Florkiewicz and Kubzdela 2013, Sloan 2013, Terzi and Selcuk 2015). Nowadays realistic prediction about the deformation becomes increasingly important, particularly for concrete face rockfill dams (Hunter and Fell 2003, Seo *et al*. 2009, Modares and Quiroz 2015, Zhang *et al*. 2015) and for high embankments for airports or high-speed railway in mountain areas (Soriano and Sanchez 1999, Nagahara *et al*. 2004, Xu *et al*. 2009, Canizal *et al*. 2015). Finite element or finite difference analysis is usually adopted for deformation prediction (Duncan 1996, Costa and Alonso 2009, Kovacevic *et al*. 2013, Alonso *et al*. 2015, Zhou *et al*. 2016), which requires developing suitable constitutive models to represent the behavior of rockfills observed in experimental study, including the non-linear stress-strain relationship, the stress-dependence of the stiffness, the non-linear strength behavior, and the intense shearing contraction and dilatancy.

Duncan and Chang (1970) proposed a hyperbolic elastic model to simulate the non-linear

*Corresponding author, Associate Professor, E-mail: mingxu@mail.tsinghua.edu.cn
[a]Professor, E-mail: songex@mail.tsinghua.edu.cn
[b]Ph.D. Student, E-mail: jdh14@mails.tsinghua.edu.cn

http://www.techno-press.org/?journal=gae&subpage=7 ISSN: 2005-307X (Print), 2092-6219 (Online)

stress-strain behavior of soils. This simple model has been widely used in engineering practice and extensive experience has been gained (e.g., Li *et al.* 2016). However, it cannot reproduce the volumetric behavior of rockfill correctly, particularly the shearing dilatancy before the peak strength under low confining pressure and continuing contraction under high confining pressure, because it is based on generalized Hooke's law. To overcome the limitations of elastic models, elastoplastic models have been developed for rockfills during the past decades (Varadarajan *et al*. 2006, Liu and Zou 2012, Indraratna *et al*. 2014, Xiao *et al*. 2014), intended to achieve more realistic prediction in numerical analysis but with the expense of increasing complexity. Xu and Song (2009) proposed a strain hardening model for rockfills, which was shown to reproduce the observed shear behavior of rockfills with fair accuracy. The model has the advantage of simplicity, and all parameters can be derived from a set of large-scale triaxial tests, which is important for engineering practice.

However, those advanced constitutive models for rockfills were seldom calibrated against the results of stress-path triaxial tests on rockfills. The main reason is simply because there was little reported research on the shear behavior of rockfill along other loading paths except for those with constant confining pressures. Because of the large particle size, large-scale triaxial apparatus are required to investigate the stress-strain behavior and strength characteristics of rockfill (e.g., Charles and Watts 1980, Nair and Latha 2012, Indraratna *et al*. 2015, Alonso *et al.* 2016). The diameter of rockfill specimen is usually 300 mm, but could be as large as 1 m (Hu *et al*. 2011, Ovalle *et al*. 2014), so that the particle size and grading of rockfills tested in the laboratory could be comparable to those in the field. A large pressure chamber as well as a high loading capacity is required, and the whole system becomes much more complicated compared to a conventional triaxial apparatus for a specimen with a diameter of 30 mm-100 mm. It is therefore expensive and difficult to build such a large apparatus and carry out testing. As a result, only a limited number of large-scale triaxial apparatuses have been built around the world, while most were designed to operate with a constant cell pressure. Thus, in previous laboratory investigations rockfill specimens were usually loaded with a constant cell pressure.

However, the stress-strain behavior of soil is in general dependent on the loading-path. The stress-path-dependent behavior has been investigated extensively for fine grain soils such as sand and clay (e.g., Bishop and Wesley 1975, Lade and Duncan 1975, Xu *et al*. 2007a, 2007b, Gasparre *et al*. 2014, Sun *et al*. 2015). Due to the lack of related research on rockfills, there are great uncertainties about their behavior along more general stress paths, which further impose uncertainties on the development of constitutive models.

To overcome such uncertainties and to further calibrate the proposed constitutive model, the authors performed a series of large-scale triaxial tests on limestone rockfill specimens, which were loaded along different stress paths (Xu *et al*. 2012). The large-scale triaxial apparatus in Tsinghua University was used. The control software and servo-control unit were designed capable of varying the deviator force and the cell pressure at pre-specified rates independently and simultaneously, so that desired stress paths could be achieved with fair accuracy. Test procedure and major findings were reported in details by Xu *et al*. (2012). Further stress-path testing on granite rockfill specimens was reported by Yang *et al*. (2010). The results of those tests reveal that the stress-strain behavior and volumetric behavior of rockfill are significantly influenced by the loading paths as well as the confining pressures.

The aim of this paper is to evaluate the capability of the strain hardening model proposed by Xu and Song (2009) to predict the shear behavior of rockfills along various stress paths. All parameters are derived entirely from conventional large triaxial tests with constant confining pressures. The predicted stress-strain and volumetric behavior along other loading paths are compared with laboratory test results. The key parameter of this model, ϕ_{v0}, which is the mobilized friction angle at the lowest point of the $\varepsilon_v - \varepsilon_1$ curve, is further discussed.

2. The strain hardening model for rockfills

A brief introduction about this model is given as below, and its application to other stress paths will be evaluated in the next section.

2.1 Yield function and hardening rule

The Mohr-Coulomb yield function F can be written in terms of principal effective stresses as follows

$$F = \frac{\sigma'_1 - \sigma'_3}{2} - \frac{\sigma'_1 + \sigma'_3}{2} \sin\phi_m - c' \cos\phi_m \tag{1}$$

Compressive stresses are assumed positive. The mobilized friction angle ϕ_m is used in Eq. (1), which increases during shearing as plastic strain develops. For rockfills, c'=0 is assumed.

The deviator stress q in triaxial compression test can be expressed as a function of the axial strain ε, using the simplified hyperbolic curve, which is shown in Fig. 1, as that adopted in the hyperbolic model by Duncan and Chang (1970)

$$q = \frac{\varepsilon}{\frac{1}{E_i} + \frac{\varepsilon}{q_{ult}}} \tag{2}$$

where q_{ult} is the asymptotic value of the hyperbolic curve, and can be related to the peak compressive strength q_f by dividing by a factor of R_f: $q_{ult}=q_f/R_f$. The rockfill strength q_f can be calculated from σ'_3 and the peak friction angle ϕ_p. The nonlinear strength characteristics of rockfills can be represented as (Duncan *et al.* 2014)

$$\phi_p = \phi_0 - \Delta\phi \log(\frac{\sigma'_3}{p_a}) \tag{3}$$

where ϕ_0 is the value of ϕ_p for $\sigma'_3=p_a$, and $\Delta\phi$ is the reduction in ϕ_p for a 10-fold increase in σ'_3. p_a is the atmospheric pressure. Xu *et al*. (2012) demonstrates that stress path has only minor influence on the strength behavior of rockfill, despite of the significant effect on the stress-strain and volumetric behavior.

E_i is the initial tangent modulus, which is dependent on σ'_3 and can be expressed as

$$E_i = K p_a (\frac{\sigma'_3}{p_a})^n \tag{4}$$

The axial strain ε can be divided into elastic strain ε^e and plastic strain ε^p, i.e., $\varepsilon=\varepsilon^e+\varepsilon^p$, as shown in Fig. 1. ε^e can be estimated as: $\varepsilon^e=q/E_{ur}$, where E_{ur} is the Young's modulus during unloading-reloading, and can be related to E_i through a constant factor R_m: $E_{ur}=R_m E_i$.

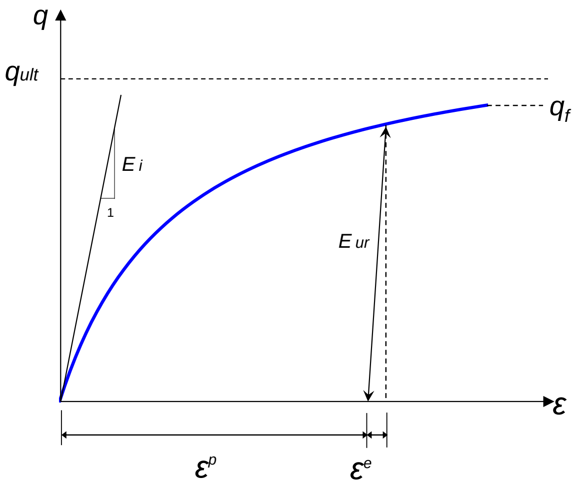

Fig. 1 The hyperbolic curve representing the non-linear stress-strain relationship of rockfills

ε^p is approximated as the plastic octahedral shear strain $\gamma_{oct}{}^p$, which is defined as

$$\gamma_{oct}{}^{p} = \frac{\sqrt{2}}{3}[(\varepsilon_1^p - \varepsilon_2^p)^2 + (\varepsilon_2^p - \varepsilon_3^p)^2 + (\varepsilon_3^p - \varepsilon_1^p)^2]^{1/2} \tag{5}$$

From the above equations, the mobilized friction angle $\phi_m = \sin^{-1}\frac{(\sigma'_1 - \sigma'_3)}{(\sigma'_1 + \sigma'_3)}$ can be finally expressed as a function of $\gamma_{oct}{}^p$. During continued loading, the mobilized friction angle ϕ_m develops as $\gamma_{oct}{}^p$ increases, resulting in isotropic hardening of the yield surface. The upper limit of ϕ_m is set to be ϕ_p, which defines the failure surface.

2.2 Flow rule

The flow rule is of non-associated type, with the plastic potential function P given by

$$P = \frac{\sigma'_1 - \sigma'_3}{2} - \frac{\sigma'_1 + \sigma'_3}{2}\sin\psi_m \tag{6}$$

The mobilized dilation angle ψ_m is used in the plastic potential function.

For sands subjected to shearing, the mobilized dilation angle ψ_m can be linked with the mobilized friction angle ϕ_m based on Rowe's stress-dilatancy theory (Rowe 1962). However, there can be significant deviations from test results when Rowe's stress-dilatancy theory is directly applied to compacted rockfills, mainly due to the pronounced influence of particle crushing. For detailed discussions one is referred to Xu and Song (2009).

Xu and Song (2009) proposed a simple solution but with fair accuracy, based on analyzing test results of different rockfills. Two parameters ϕ_{v0} and R_d are introduced and the mobilized dilation angle ψ_m is expressed as

$$\sin\psi_m = R_d \frac{\sin\phi_m - \sin\phi_{v0}}{1 - \sin\phi_m \sin\phi_{v0}} \tag{7}$$

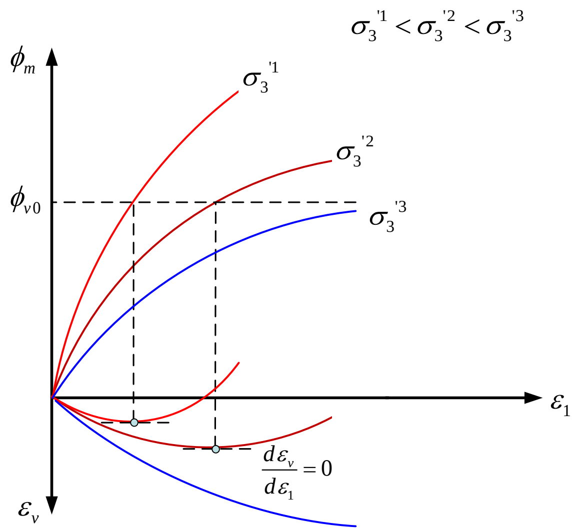

Fig. 2 ϕ_m–ε_1 and ε_v–ε_1 for rockfill specimens loaded with different confining pressures

ϕ_{v0} is the mobilized friction angle at the lowest point of the ε_v–ε_1 curve, i.e., $d\varepsilon_v/d\varepsilon_1$=0 (Fig. 2). A further improvement to the method is proposed here, as it is observed that the rockfill volume might continue to contract without obvious trend to dilate at high confining pressure. In such situation the value of ϕ_{v0} can be approximated as the peak friction angle. For convenience, a constant value of ϕ_{v0}, i.e., the average value under different confining pressures, can be taken in the calculation. R_d is introduced as an empirical factor, which can be determined by fitting the experimental data at each confining pressure. The magnitude of R_d is found to vary approximately linearly with the confining pressures, and can be further approximated as $R_d = k_1 + k_2 \frac{\sigma_3^{'}}{p_a}$, where k_1 and k_2 are two constants. By introducing ϕ_{v0} and R_d, combined with the non-linear stress-strain relationship and the non-linear strength criterion, the model can simulate the varying volumetric behavior of rockfills during shearing at different confining pressures, i.e., shearing dilatancy at low confining pressure and shearing contraction at high confining pressure, as demonstrated in Fig. 2, which is well observed in large-scale triaxial tests on rockfills. A detailed discussion will be presented in Section 4.

3. Prediction of the shear behavior of rockfills along different loading paths

The capability of the model described previously, to predict the shear behavior of rockfills along various loading paths, was evaluated by comparing predicted results with those observed in the large-scale stress-path triaxial tests, which were performed by Xu *et al*. (2012) and Yang *et al*. (2010) on limestone rockfill specimens and granite rockfill specimens, respectively. The strain-hardening model was implemented in the finite difference program FLAC, by modifying the in-built Mohr-Coulomb model, using the embedded language FISH (Itasca 2005). The model parameters were derived entirely from the results of tests with constant confining pressures, i.e., conventional large triaxial tests. Next, the parameters were used to predict the stress-strain and volumetric behavior of the rockfills subjected to various loading paths. The predicted results were compared with those observed in the laboratory.

3.1 Comparison with the stress-path test results by Xu et al. (2012)

The tests were performed in the large-scale triaxial apparatus in Tsinghua University, as shown in Fig. 3. The quarried limestone rockfill tested in this research consists of angular particles with a light grey color. The rockfills were taken from the construction site of the high embankment under the runway for Kunming New International Airport in south-western China. The maximum height of the embankment is 54 m. The specimens had a diameter of 300 mm and a height of 730 mm. The dry density of the specimens was 20.5 kN/m^3. Specimens were fully saturated before consolidation to the specified isotropic effective stress, followed by monotonic compression to failure in drained condition along different loading paths, including constant lateral effective stress σ_3', constant mean effective stress $p'=(\sigma_1'+2\sigma_3')/3$, and constant vertical effective stress σ_1'. Detailed description about the rockfills and testing procedure can be found in Xu *et al*. (2012).

The parameters for the simulation were derived entirely from the results of conventional large triaxial tests with constant σ_3'. The strength parameters (ϕ_0, $\Delta\phi$, R_f) and stiffness parameters (K, n, R_m) are identical to those for the Duncan and Chang model, and were derived following the procedure described by Duncan and Chang (1970). The three parameters for the flow rule, ϕ_{v0}, k_1 and k_2, were derived following the procedure described by Xu and Song (2009). The parameters thus determined are summarized in Table 1. These parameters were adopted in the model to simulate the conventional large triaxial tests. As shown in Fig. 4, fair consistence was found between the calculated results and the experimental results. Of particular interest is that the effect of confining pressure on the volumetric behavior was reproduced. At low confining pressure, the rockfill volume contracted initially, followed by dilation at large strains; while at high confining pressure, significant contractive strain continued to develop, which could be a result of more particle breakage (Zhang *et al*. 2013).

The same parameters were adopted to calculate the shear behavior along other loading paths. Although the modeling was performed after the publication of the test results, such simulation can be deemed as a “genuine” prediction about the behavior along other loading paths because the parameters were derived entirely from the results of conventional large triaxial tests with constant σ_3'.

Fig. 3 The large-scale triaxial apparatus in Tsinghua University

The predicted results are compared with the experimental results. Fig. 5 shows the predicted and observed stress-strain and volumetric behavior of three specimens sheared at the same initial isotropic effective stress state p'_0=1000 kPa, but along three different stress paths in the p'-q space, i.e., constant σ'_3, constant p', and constant σ'_1, as shown on the insert. The effect of loading direction on the volumetric response is highlighted. When the loading direction varied from constant σ'_3 to constant σ'_1, more dilative strain was observed.

Fig. 6 shows the results of two specimens loaded at different p'_0, but along the same loading direction with constant p'. Similar to the observations in previous Fig. 4, here a higher mean effective stress also led to more contractive behavior. As can be seen from Figs. 5 and 6, the predicted results compare fairly well with the experimental results, not only for the stress-strain behavior but also for the volumetric behavior. It is interesting to note that the model was originally developed, based on observations of conventional triaxial tests, in which the confining pressure was kept constant, while the confining pressure was varying during loading along other stress paths.

However, some discrepancies do exist. The prediction did not reproduce the slight strain softening behavior for the specimens loaded with constant p' and with constant σ'_1. This is because the model in its current form does not aim to simulate the post-failure behavior of compacted rockfills. But it is possible to implement isotropic softening of yield surface after reaching the peak strength during further development of the model. Furthermore, more contractive volumetric strains were predicted (Figs. 5 and 6). However, those differences are relatively small, particularly for engineering practice.

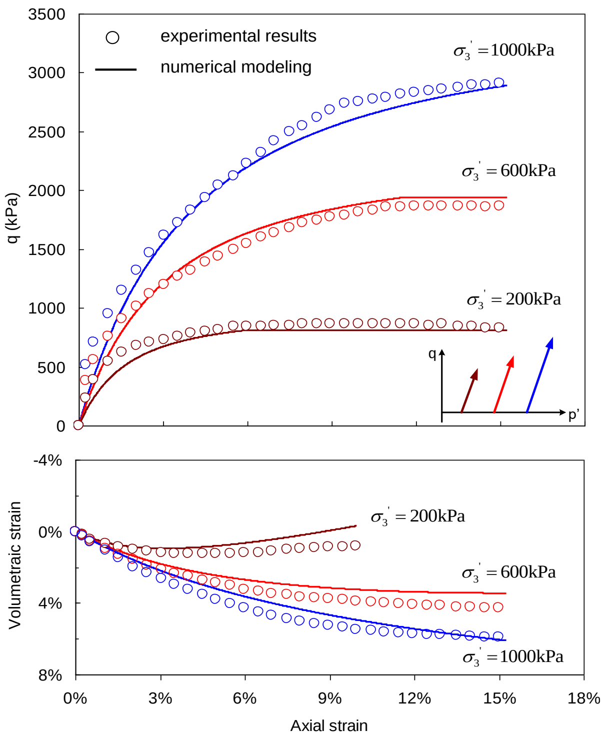

Fig. 4 Comparison between numerical simulation and experimental results for limestone rockfill specimens loaded with constant confining pressures

Table 1 Parameters for the limestone rockfill

ϕ_0	$\Delta\phi$	R_f	K	n	v	R_m	ϕ_{v0}	k_1	k_2
44.54	8.26	0.83	587.75	0.2963	0.3	5	39.0	1.1425	0.0412

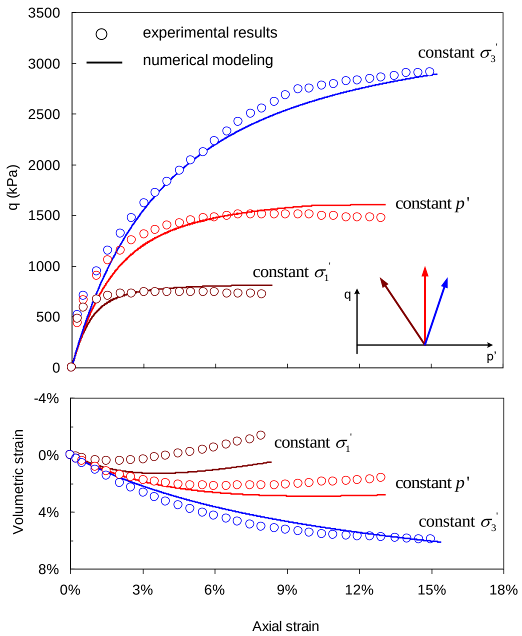

Fig. 5 Comparison between numerical simulation and experimental results for limestone rockfill specimens loaded from p_0'=1000 kPa along different loading paths

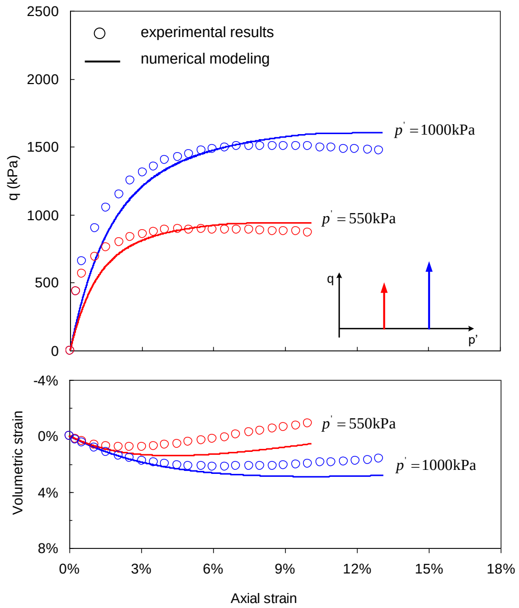

Fig. 6 Comparison between numerical simulation and experimental results for limestone rockfill specimens loaded with constant p'

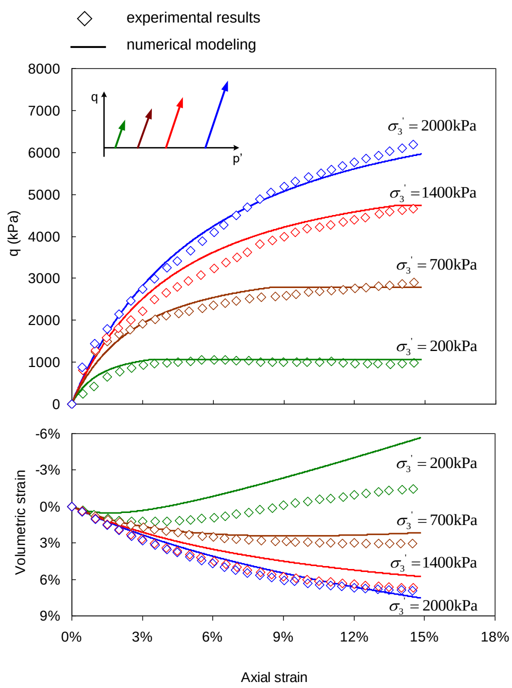

Fig. 7 Comparison between numerical simulation and experimental results for granite rockfill specimens loaded with constant confining pressures

Table 2 Parameters for the granite rockfill

ϕ_0	$\Delta\phi$	R_f	K	n	ν	R_m	ϕ_{v0}	k_1	k_2
49.27	9.02	0.8	1225	0.15	0.3	5	42.0	1.21	0.0138

3.2 Comparison with the stress-path test results by Yang et al. (2010)

The tests were also performed in the same large-scale triaxial apparatus in Tsinghua University. The granite rockfills specimens had a dry density of 19.8 kN/m^3. After isotropic consolidation, the specimens were loaded in drained condition with constant σ_3' or with constant p'. Each shearing test consisted of initial monotonic compression, followed by an unloading-reloading loop at large strains along the same stress path. The results of the initial monotonic compression were used in this investigation.

The parameters for the simulation were also derived only from the results of conventional large triaxial tests with constant confining pressures, and are summarized in Table 2. A comparison was made between the calculated results and those observed during four conventional large triaxial tests, as shown in Fig. 7. Fair consistence was found, though more volumetric dilatation was calculated at large strains for the specimen sheared with the lowest confining pressure (σ_3'=200 kPa).

Simulations with the same parameters were carried out, to predict the response of other four specimens, which were loaded at different initial isotropic stress states, but along the same loading direction with constant p'. As shown in Fig. 8, the influence of the mean effective stress on both the stress-strain relationship and the volumetric behavior was predicted with reasonable accuracy.

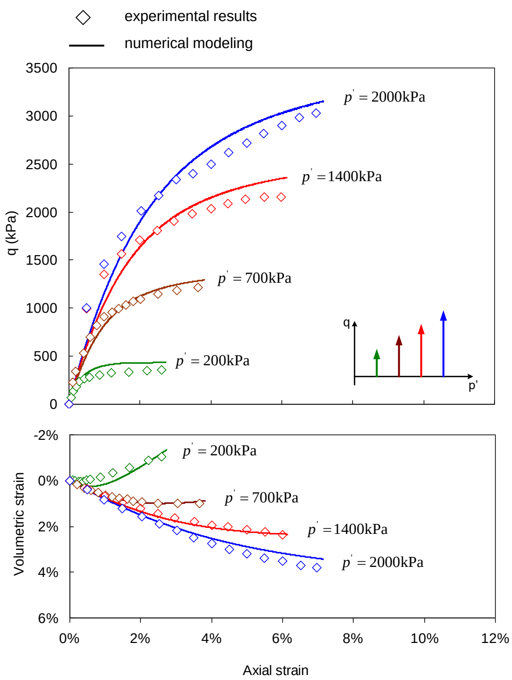

Fig. 8 Comparison between numerical simulation and experimental results for granite rockfill specimens loaded with constant p'

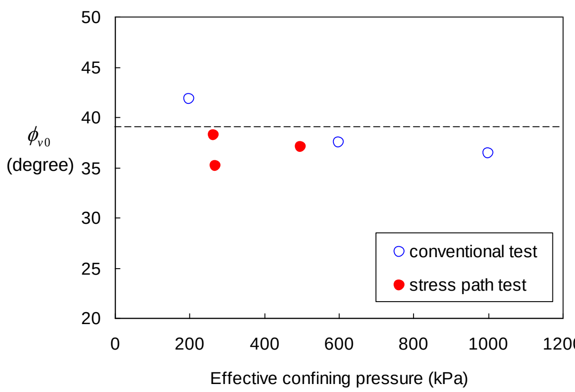

(a) ϕ_{v0} for the limestone rockfill

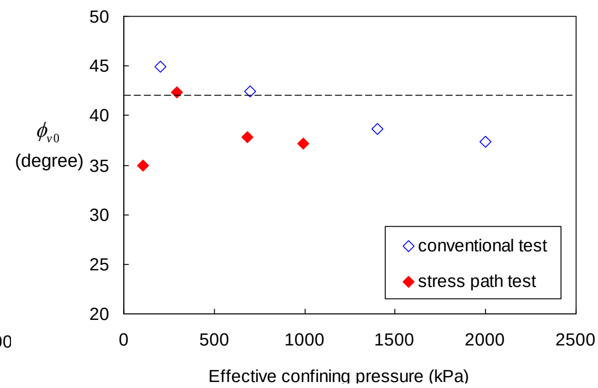

(b) ϕ_{v0} for the granite rockfill

Fig. 9 Variation of ϕ_{v0} with corresponding confining pressures for conventional tests and stress path tests

4. Discussion

To reproduce the complex shear behavior of rockfills, Rowe's stress dilatancy theory is revised by proposing the mobilized friction angle ϕ_{v0} and Eq. 7, so that the stress-dependent stress-strain behavior, the stress-dependent strength behavior, and the stress-dependent volumetric behavior can be integrated in this simple model without requiring too many parameters. The mobilized friction angle, at which the volumetric behavior is changing from contraction to dilation, is defined as ϕ_{v0}

(Xu and Song 2009). This mobilized friction angle ϕ_{v0} is introduced as an important parameter to link the mobilized friction angle to the mobilized dilation angle of rockfills.

The values of the mobilized friction angle ϕ_{v0} for the limestone rockfill and the granite rockfill in the conventional large triaxial tests by Xu *et al*. (2012) and Yang *et al*. (2010) are plotted against the effective confining pressure σ_3' in Figs. 9(a) and 9(b), respectively. For those two rockfills loaded at higher confining pressures, the volume continued to contract without obvious dilation, i.e., tests with σ_3'=600 kPa and 1000 kPa by Xu *et al*. (2012), and tests with σ_3'=1400 kPa and 2000 kPa by Yang *et al*. (2010). In such situation, the value of ϕ_{v0} was approximated as the mobilized friction angle at large strain (about 15%) at the end of the test, which was the peak friction angle. The error was expected to be small as both curves of ϕ_m–ε_1 and ε_v–ε_1 became relatively flat at large strain. In contrast, Xu and Song (2009) noticed that both the quarried rockfill and the alluvial rockfill tested by Varadarajan *et al*. (2006) showed dilatant behavior after initial contraction during shearing at all confining pressures.

As can be seen from Figs. 9(a) and 9(b), the values of ϕ_{v0} of those two rockfills in conventional large triaxial tests seem to decrease with increasing confining pressure. This is different from the previous observation by Xu and Song (2009), in which the values of ϕ_{v0} of two rockfills were found relatively constant at different confining pressures, though the quarried rockfill showed a higher value of ϕ_{v0} at a low σ_3'=300kPa. Therefore, a more generalized conclusion about the dependency of the mobilized friction angle ϕ_{v0} on the confining pressure needs further exploration on existing experimental data of conventional large triaxial tests on different rockfills.

The values of the mobilized friction angle ϕ_{v0} are also derived from large triaxial stress path tests, and are plotted against the corresponding confining pressures in the same figure. More scatter is observed, and it is difficult to define a clear link with the confining pressure due to the limited number of tests. However, the values of ϕ_{v0} for stress path tests seem to be located below those for conventional tests, indicating that a smaller mobilized strength is required to dilate during shearing along those two stress paths, i.e., constant p' and constant σ_1'. It is interesting to note that a relatively shorter distance towards the failure envelope is required along those two stress paths, compared to that for a conventional test with constant σ_3'. Thus this observation also demonstrates the influence of the loading path direction on the deformation behavior of rockfills. Further laboratory investigation is required to identify the interlink among the values of ϕ_{v0}, the corresponding confining pressure, and the stress path, since there are only very limited large triaxial tests performed along other stress paths.

As a simplification, a constant value of ϕ_{v0} is adopted in the model, as plotted as the dashed line in Figs. 9(a) and 9(b). In general, satisfactory predictions are observed for both conventional tests and stress path tests (Figs. 4-8). The simulation results were found not to be too sensitive to the variation of this parameter, mainly because the slope of the ε_v–ε_1 curve is relatively flat at its lowest position and thus a variation of ϕ_{v0} by a few degrees would not induce large difference to the results. Furthermore, though the value of ϕ_{v0} is constant, it can still imposes influence on the volumetric behavior at different confining pressures, as the confining pressure determines the non-linear stress-strain behavior and non-linear strength envelope of rockfills. A lower confining pressure leads to a higher peak friction angle and thus a higher curve of mobilized friction angle against axial strain (ϕ_m–ε_1). As a result, less axial strain is required to reach the same mobilized friction angle at lower confining pressure, indicating a quicker initiation of the dilation. If the peak friction angle at high confining pressure is smaller than the specified value of ϕ_{v0}, the volume will continue to contract with a decreasing rate, as shown in Fig. 2.

Compared with other advanced constitutive models for rockfills, the proposed model has the advantage of simplicity, which makes it attractive for routine design. The model can be easily implemented into a commercial finite element or finite difference program by modifying the existing Mohr-Coulomb model, in which the friction angle as well as the dilation angle is not specified as a constant, but is expressed as a function of the plastic octahedral shear strain and continues to be updated during the process of loading. Ten parameters are required (Table 1), among which seven parameters are identical to those for a hyperbolic model, while the other three (ϕ_{v0}, k_1, k_2) can be derived from the same set of large triaxial tests. As shown previously, despite of its simplicity, the model has proven to be able to predict the shear characteristics of rockfills with fair accuracy, not only for conventional tests but also for stress path tests.

There are also limitations with this model at its current version. As isotropic hardening is assumed, no plastic strain is predicted during unloading and reloading. However, the error is expected to be small for many engineering problems. Another limitation is that only elastic behavior occurs during proportional loading, e.g., K_0 loading. Further improvement can be made by introducing a cap yield surface.

5. Conclusions

Experimental study reveals that compacted rockfills show a significant stress-path-dependent behavior during loading, which is more complicated than the behavior of sand due to the influence of the confining pressures on the volumetric behavior and strength behavior. Therefore a realistic prediction of deformation of rockfill structures requires constitutive models to properly reproduce such behavior. This paper evaluates the capability of a strain hardening model proposed by the authors. Despite of its simplicity, essential aspects of the shear behavior of rockfills can be simulated, including the non-linear stress-strain relationship, the stress-dependence of the stiffness, the non-linear strength behavior, and in particular the shear contraction and dilatancy. Compared with large-scale triaxial stress-path test results, the model has shown to predict the significant different stress-strain and volumetric behavior along various loading paths with fair accuracy. All parameters required for the model can be derived entirely from the results of conventional large triaxial tests with constant confining pressures.

Acknowledgments

The work presented in this paper is part of a research project funded by the National Natural Science Foundation of China (41272280) and China 973 Program (2014CB047003), the support of which are gratefully acknowledged by the authors.

References

Alonso, E.E., Olivella, S., Soriano, A., Pinyol, N.M. and Esteban, F. (2015), "Modelling the response of Lechago earth and rockfill dam", *Géotechnique,* **61**(5), 387-407.

Alonso, E.E., Romero, E. and Ortega, E. (2016), "Yielding of rockfill in relative humidity-controlled triaxial experiments", *Acta Geotechnica,* **11**(3), 455-477.

Bishop, A.W. and Wesley, L.D. (1975), "A hydraulic triaxial apparatus for controlled stress path testing",

Géotechnique, **25**(4), 657-670.
Canizal, J., Castro, J., Costa, A.D., Sagaseta, C. and Sola, P. (2015), "High rockfill embankment for the extension of an airport main runway", *Proceedings of the 15th Pan-American Conference on Soil Mechanics and Geotechnical Engineering*, Buenos Aires, Argentina, December.
Charles, J.A. (2008), "The engineering behaviour of fill materials, the use, misuse and disuse of case histories", *Géotechnique*, **58**(7), 541-570.
Charles, J.A. and Watts, K.S. (1980), "The influence of confining pressure on the shear strength of compacted rockfill", *Géotechnique*, **30**(4), 353-367.
Costa, L.M. and Alonso, E.E. (2009), "Predicting the behavior of an earth and rockfill dam under construction", *J. Geotech. Geoenviron. Eng.*, **135**(7), 851-862.
Duncan, J.M. (1996), "State of the art, limit equilibrium and finite-element analysis of slopes", *J. Geotech. Eng.*, **122**(7), 577-596.
Duncan, J.M. and Chang, C.Y. (1970), "Nonlinear analysis of stress and strain in soils", *J. Soil. Mech. Found. Div.*, **96**(5), 1629-1653.
Duncan, J.M., Wright, S.G. and Brandon, T.L. (2014), *Soil Strength and Slope Stability*, John Wiley and Sons.
Florkiewicz, A. and Kubzdela, A. (2013), "Factor of safety in limit analysis of slopes", *Geomech. Eng.*, **5**(5), 485-497.
Gasparre, A., Hight, D.W., Coop, M.R. and Jardine, R.J. (2014), "The laboratory measurement and interpretation of the small-strain stiffness of stiff clays", *Géotechnique*, **64**(12), 942-953.
Griffiths, D.V. and Marquez, R.M. (2007), "Three-dimensional slope stability analysis by elasto-plastic finite elements", *Géotechnique*, **57**(3), 537-546.
Hu, W., Dano, C., Hicher, P.Y., Touzo, J.Y.L., Derkx, F. and Merliot, E. (2011), "Effect of sample size on the behavior of granular materials", *ASTM Geotech. Test. J.*, **34**(3), 186-197.
Hunter, G. and Fell, R. (2003), "Rockfill modulus and settlement of concrete face rockfill dams", *J. Geotech. Geoenviron. Eng.*, **129**(10), 909-917.
Indraratna, B., Nimbalkar, S., Coop, M. and Sloan, S.W. (2014), "A constitutive model for coal-fouled ballast capturing the effects of particle degradation", *Comput. Geotech.*, **61**, 96-107.
Indraratna, B., Sun, Q. and Nimbalkar, S. (2015), "Observed and predicted behaviour of rail ballast under monotonic loading capturing particle breakage", *Can. Geotech. J.*, **52**(1), 73-86.
Itasca (2005), *User's Guide for FLAC Version 5.0*.
Kovacevic, N., Hight, D.W., Potts, D.M. and Carter, I.C. (2013), "Finite-element analysis of the failure and reconstruction of the main dam embankment at Abberton Reservoir, Essex, UK", *Géotechnique*, **63**(9), 753-767.
Lade, P.V. and Duncan, J.M. (1975), "Stress-path dependent behaviour of cohesionless soil", *J. Geotech. Eng. Div.*, **102**(1), 51-68.
Li, S., Yu, S., Shangguan, Z. and Wang, Z. (2016), "Estimating model parameters of rockfill materials based on genetic algorithm and strain measurements", *Geomech. Eng.*, **10**(1), 37-48.
Liu, H. and Zou, D. (2012), "Associated generalized plasticity framework for modeling gravelly soils considering particle breakage", *J. Eng. Mech.*, **139**(5), 606-615.
Modares, M. and Quiroz, J.E. (2015), "Structural analysis framework for concrete-faced rockfill dams", *J. Geomech.*, **16**(1), 04015024.
Nagahara, H., Fujiyama, T., Ishiguro, T. and Ohta, H. (2004), "FEM analysis of high airport embankment with horizontal drains", *Geotext. Geomembr.*, **22**(2), 49-62.
Nair, A.M. and Latha, G.M. (2012), "Taming of large diameter triaxial setup", *Geomech. Eng.*, **4**(4), 251-262.
Ovalle, C., Frossard, E., Dano, C., Hu, W., Maiolino, S. and Hicher, P.Y. (2014), "The effect of size on the strength of coarse rock aggregates and large rockfill samples through experimental data", *Acta Mech.*, **225**(8), 2199-2216.
Rowe, P.W. (1962), "The stress-dilatancy relation for static equilibrium of an assembly of particles in contact", *Proceedings of the Royal Society*, **269**, 500-527.

Seo, M.W., Ha, I.S., Kim, Y.S. and Olson, S.M. (2009), "Behavior of concrete-faced rockfill dams during initial impoundment", *J. Geotech. Geoenviron. Eng.*, **135**(8), 1070-1081.
Sloan, S.W. (2013), "Geotechnical stability analysis", *Géotechnique*, **63**(7), 531-571.
Soriano, A. and Sanchez, F.J. (1999), "Settlements of railroad high embankments", *Proceedings of the 12th European Conference on Soil Mechanics and Geotechnical Engineering*, Amsterdam, Netherlands, June.
Sun, D., Chen, L., Zhang, J. and Zhou, A. (2015), "Bifurcation analysis of over-consolidated clays in different stress paths and drainage conditions", *Geomech. Eng.*, **9**(5), 669-685.
Terzi, N.U. and Selcuk, M.E. (2015), "Nonlinear dynamic behavior of pamukcay earthfill dam", *Geomech. Eng.*, **9**(1), 83-100.
Varadarajan, A., Sharma, K.G., Abbas, S.M. and Dhawan A.K. (2006), "Constitutive model for rockfill materials and determination of material constants", *J. Geomech.*, **6**(4), 226-237.
Xiao, Y., Liu, H., Chen, Y., Jiang, J. and Zhang, W. (2014), "State-dependent constitutive model for rockfill materials", *J. Geomech.*, **15**(5), 04014075.
Xu, M., Bloodworth, A. and Clayton, C.R.I. (2007a), "Behavior of a stiff clay behind embedded integral abutments", *J. Geotech. Geoenviron. Eng.*, **133**(6), 721-730.
Xu, M., Clayton, C.R.I. and Bloodworth, A. (2007b), "The earth pressure behind full-height frame integral abutments supporting granular backfill", *Can. Geotech. J.*, **44**(3), 284-298.
Xu, M. and Song, E. (2009), "Numerical simulation of the shear behavior of rockfills", *Comput. Geotech.*, **36**(8), 1259-1264.
Xu, M., Song, E. and Cao, G. (2009), "Compressibility of broken rock-fine grain soil mixture", *Geomech. Eng.*, **1**(2), 169-178.
Xu, M., Song, E. and Chen, J. (2012), "A large triaxial investigation of the stress-path-dependent behavior of compacted rockfill", *Acta Geotech.*, **7**(3), 167-175.
Yang, G., Sun, X., Yu, Y. and Zhang, B. (2010), "Experimental study of mechanical behavior of a coarse-grained material under various stress paths", *Rock Soil Mech.*, **31**(4), 1118-1122.
Zhang, B., Jie, Y. and Kong, D. (2013), "Particle size distribution and relative breakage for a cement ellipsoid aggregate", *Comput. Geotech.*, **53**, 31-39.
Zhang, J.M., Yang, Z., Gao, X. and Zhang, J. (2015), "Geotechnical aspects and seismic damage of the 156-m-high Zipingpu concrete-faced rockfill dam following the Ms 8.0 Wenchuan earthquake", *Soil Dyn. Earthq. Eng.*, **76**, 145-156.
Zhou, W., Li, S., Ma, G., Chang, X. and Cheng, Y. (2016), "Assessment of the crest cracks of the Pubugou rockfill dam based on parameters back analysis", *Geomech. Eng.*, **11**(4), 571-585.

GC